Avalanche detectors in 110nm CMOS for high-energy radiation imaging and sub-nanosecond timing

Lucio Pancheri[1,2*], Jacopo Endrizzi[1,2], Thomas Corradino[2,3], Umberto Follo[4,6], Giulia Gioachin[5,6], Chiara Ferrero[4,6], Marco Mandurrino[6], Manuel Da Rocha Rolo[6], Stefania Bufalino[5,6], Angelo Rivetti[6],

[1]DII, Università di Trento, Trento, Italy, [2]TIFPA-INFN, Trento, Italy, [3]FBK, Trento, Italy,
[4]DET, Politecnico di Torino, Torino, Italy, [5]DISAT, Politecnico di Torino, Torino, Italy, [6]INFN Torino, Torino, Italy
[*]*Corresponding author: phone: +39 0461 281532, e-mail: lucio.pancheri@unitn.it*

Abstract

This contribution presents avalanche detectors fabricated in a customized 110nm CMOS process for high-energy radiation imaging applications. The devices, operating at low gain in sub-Geiger mode, can be integrated in arrays, and provide charge collection and avalanche multiplication for charge generated in the whole pixel volume. The structure of test devices having an active thickness of 48µm is presented, along with a summary of key electrical and functional characterization results.

Introduction

The detection of high-energy charged particles and photons in several fundamental and applied physics experiments increasingly demands cost-effective large-area sensors with enhanced timing resolution and low power consumption. To meet these requirements, signal amplification by impact ionization can be a viable solution, and hybrid avalanche detectors are currently studied for both charged particles and soft X-rays imaging [1,2]. While monolithic APD arrays, operating both in Geiger and sub-Geiger mode, have been widely explored both by the academia and by image sensors manufacturers [3-5], thick monolithic avalanche detectors integrated in CMOS processes suitable for High Energy radiation imaging are not readily available for mass production. This work presents ongoing efforts to adapt the 110nm CMOS fully depleted monolithic sensor technology developed under the INFN ARCADIA project [6] by integrating a gain layer under the readout electrodes. This will provide monolithic avalanche pixels operated in sub-Geiger mode with thick depleted active area, as a cost-effective solution for high-energy particles and photons imaging and timing with sub-ns resolution.

Device Description

A cross-section of the proposed sensor is shown in Figure 1. The sensor's active region consists of a high-resistivity n-type epitaxial layer grown on a standard p+-doped silicon substrate. The thickness of the epitaxial layer is adjustable. A sufficiently high voltage applied to the top electrode depletes the gain layer, requiring a bias resistor and AC coupling to the low-voltage readout electronics. The substrate must be biased at a negative voltage to deplete the entire active volume and generate the necessary drift field. Deep pwells are implanted below the electronics and serve a two-fold purpose. Firstly, they prevent charge collection by the nwell in the inter-pixel area, which is necessary for integrating pMOS transistors in the pixels. Secondly, deep pwells extending towards the gain layer generate a horizontal electric field. This field drives electrons generated in the inter-pixel regions towards the collection electrodes, enabling charge collection and multiplication from the entire active volume (Figure 2).

Experimental Data

A wafer lot was produced to test this concept, with the main goal of developing monolithic sensors for Time-of-Flight layers in ALICE 3 detector upgrade at CERN [7]. The first design iterations, using an active layer thickness of 48µm, include multiple test pixel layouts, exploring large pixels optimized for timing resolution and structures with smaller pixels suited for combined tracking and timing (Figures 3 and 4).

Additionally, a sensor array with integrated readout electronics was developed using 250×80 μm^2 pixels. Different splits of the gain implantation dose were tested on different wafers to optimize the avalanche field experimentally.
Electrical and electro-optical characterizations were carried out on test devices. I-V curves measured in the dark are shown in Figure 5 for devices with 3 different gain implantation doses and without gain implant. I-V curves were also measured with top-side illumination using an Infrared LED at 850nm. Gain-voltage curves for the same devices, calculated as the ratio of photocurrent measured on devices with and without the gain layer implant, are shown in Figure 6. Depending on the gain dose split, the sensors exhibit a gain ranging from 5 to 30 when biased at 35 – 45V, with the backside biased between -25 and -30V. This ensures full depletion of the 48-µm active volume and a drift field strong enough for fast charge collection, of the order of 1ns, throughout the volume.
Capacitance-Voltage curves are shown in Figure 7 on a test structure featuring an array of 400 pixels connected in parallel. The optical pulse response of the test devices was obtained using an infrared picosecond pulsed laser at 1060nm and amplifying the output signal using a 2-GHz amplifier. The signal acquired from one of the test arrays with the top electrode biased at different voltages is shown in Figure 8.

TCAD Simulations

The uniformity of avalanche gain and signal timing within the sensor volume is currently under investigation, both in simulation and experimentally. Figure 9 shows the simplified cross-section of a 3-pixel domain used in TCAD simulations to study gain and timing response uniformity. In this domain, the response to a high-energy charged particle is simulated with a uniform generation along a line perpendicular to the device surface and crossing the whole detector area, while the response to X-rays considers electron-hole pair generation in a small volume located in different parts of the device.
Simulations show that the avalanche gain changes as a function of radiation incidence position both horizontally and vertically (Figure 10). However, the gain dependence on position can be modified by varying the extension of the deep pwell edge towards the gain layer. This allows for fine-tuning to achieve a maximally flat gain-position curve along the device.
Event timing is also affected by the position where the charged particle or the photon is absorbed. Transient signals simulated with photons absorbed at different horizontal and vertical positions within the device are shown in Figures 11 and 12. As can be observed, for high-energy photons a shift in the signal rising edge of almost 1ns is present between the situation where the photon is absorbed in the center of a pixel close to the collection electrode and in the region between two pixels towards the bottom of the active volume. It should be mentioned, however, that in the case of charged particles the non-uniformity of the rising edge position is mitigated, since the generation occurs in the entire active thickness.
Experimental studies of gain non-uniformity within pixels, both with charged particles and with photons, are currently in progress, as well as activities to characterize the uniformity of the detectors over large areas and on different wafers.

Acknowledgments

We would like to thank LFoundry for the support in the customization of their 110nm CMOS process.

References

[1] P. Svihra, et. al., JINST Vol. 19, C11006, 2024. https://doi.org/10.1088/1748-0221/19/11/C11006
[2] N. Cartiglia, et al., NIMA Vol. 1040, 167228, 2022. https://doi.org/10.1016/j.nima.2022.167228
[3] K. Morimoto, et al., Optica Vol. 7, No. 4, pp. 346-354, 2020. https://doi.org/10.1364/OPTICA.386574
[4] R.K. Henderson, et al., IEEE J. Solid-State Circ. Vol. 54, No. 7, 2019. https://doi.org/10.1109/JSSC.2019.2905163
[5] Y. Hirose, et al., Sensors Vol. 18, 3642, 2018. https://doi.org/10.3390/s18113642
[6] L. Pancheri, et al., IEEE Tran. Electron. Dev. Vol. 67, 2020. https://doi.org/10.1109/TED.2020.2985639
[7] ALICE collaboration, CERN-LHCC-2022-009. https://doi.org/10.48550/arXiv.2211.02491

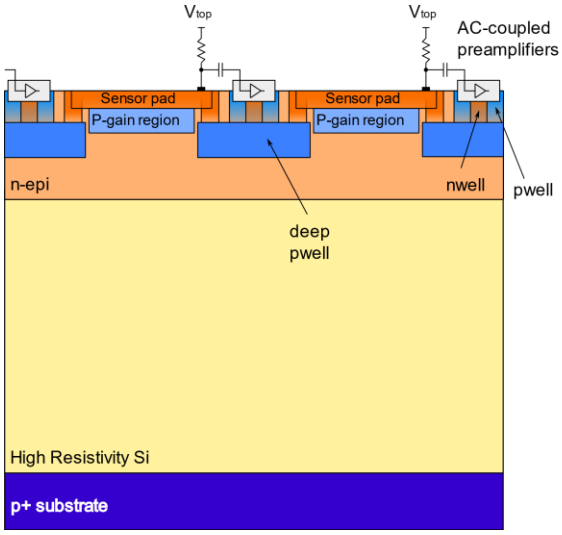

Figure 1. Schematic cross section of 2 pixels.

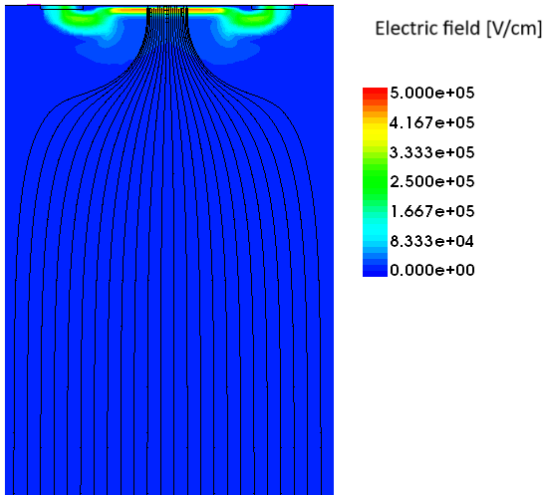

Figure 2. Electric field map of a single pixel. In the simulation, a voltage of 36V is applied at the top surface and -30V at the backside.

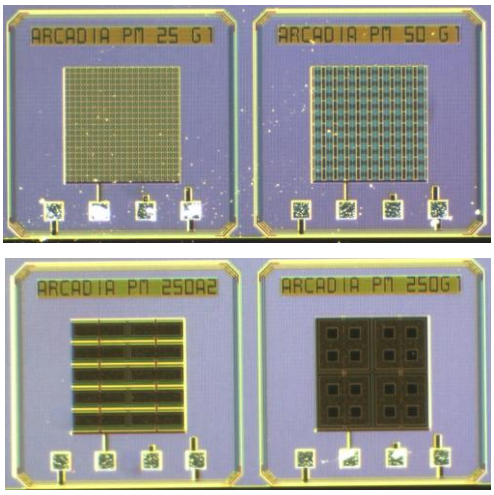

Figure 3. Micrographs of test pixel arrays with different sizes fabricated in 110nm CMOS. The pixel size in the 4 test structures is 25x25, 50x50, 250x80 and 250x250 μm^2, and the arrays active area is 0.5x0.5mm^2.

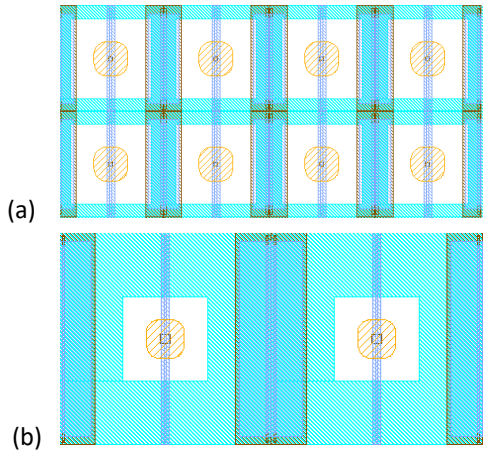

Figure 4. (a) Layout of 25x25 μm^2 test pixels. (b) Layout of 50x50 μm^2 test pixels. In both layouts the gain implantation area is shown in orange and the area available for transistors is colored in light-blue.

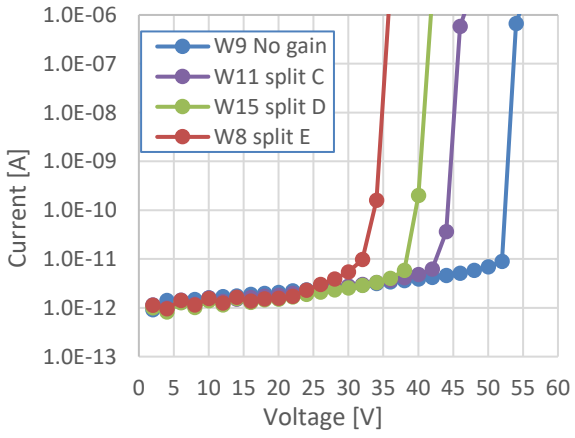

Figure 5. Current-Voltage curves measured on the 25x25 μm^2 pixel array test structures with different implanted doses.

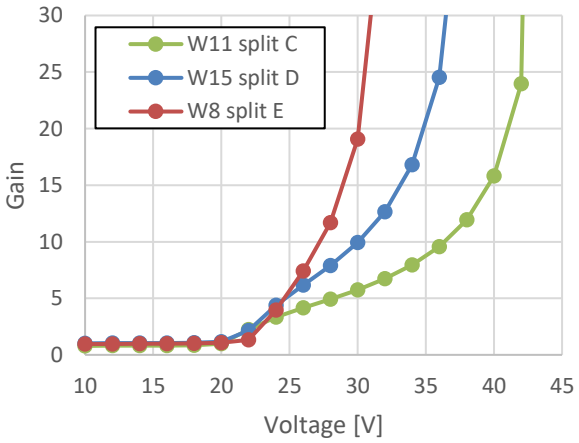

Figure 6. Avalanche gain measured on the 25x25 μm^2 pixel test structures with a DC infrared LED light (850nm) illuminating the device top surface. Gain was calculated as a ratio between currents flowing in devices with and without gain implantion.

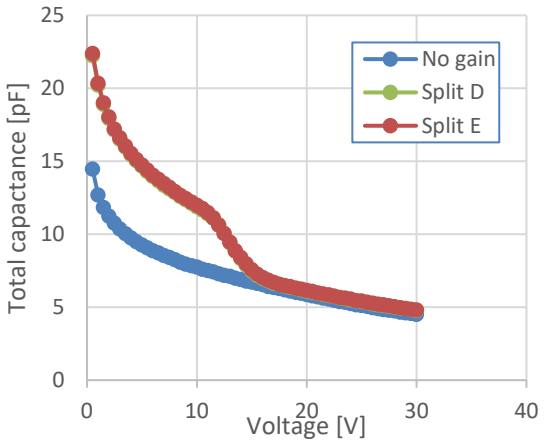

Figure 7. Capacitance-Voltage curves measured on the 25x25 µm^2 pixel array test structures.

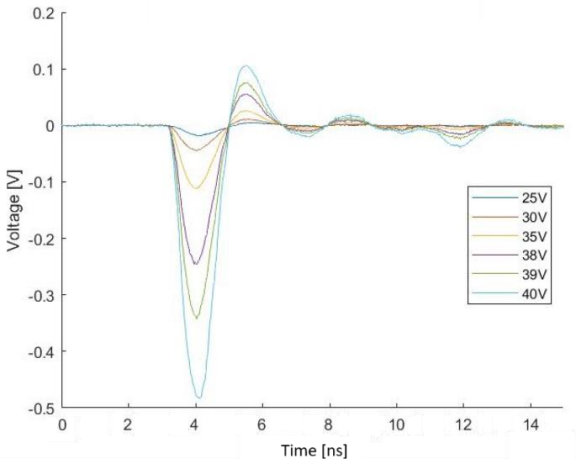

Figure 8. Signal measured on a 25x25 µm^2 pixel test structure biased at different voltages and flood illuminated with a picosecond IR laser (1060nm). The device was connected to a 2-GHz bandwidth amplifier and the signal was acquired using a 5-GHz oscilloscope.

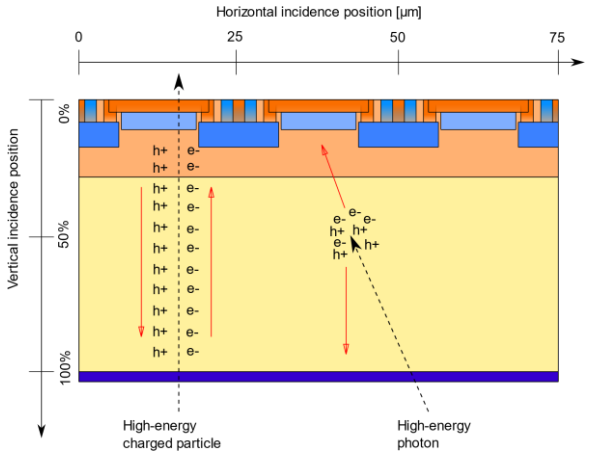

Figure 9. 3-pixel domain used in TCAD simulations, targeting the signal produced by high-energy particles and photons.

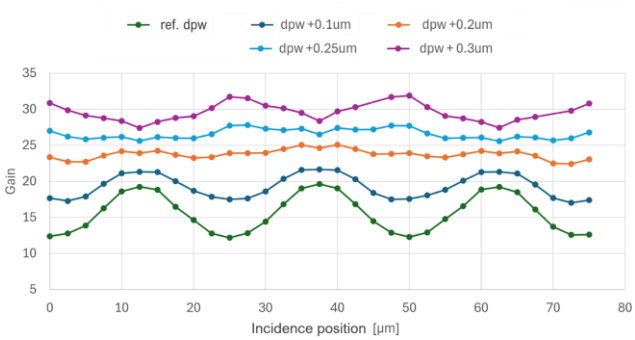

Figure 10. Avalanche gain as a function of particle incidence position for different values of deep pwell width.

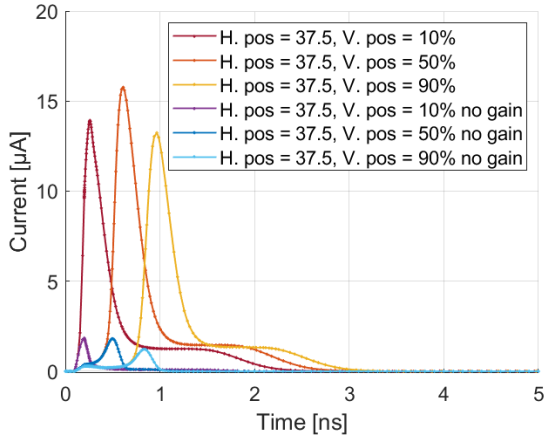

Figure 11. Transient signals produced by a high-energy photon absorbed at different depths in the center of a pixel. Sensors with and without avalanche gain implantation are compared.

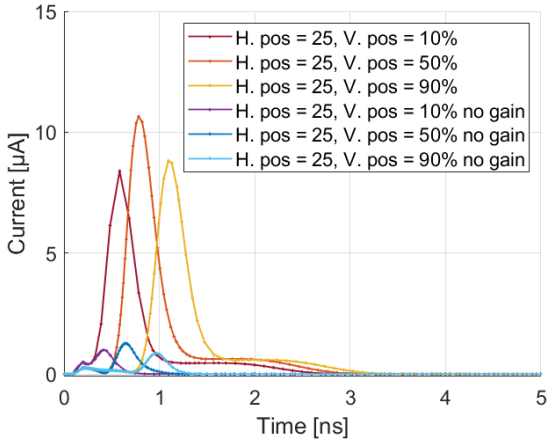

Figure 12. Transient signals produced by a high-energy photon absorbed at different depths at the boundary between two pixels. Sensors with and without avalanche gain implantation are compared.